FTIR Detection of Water Reactions during the Flash-Induced S-State Cycle of the Photosynthetic Water-Oxidizing Complex†

Takumi Noguchi*,‡ and Miwa Sugiura§

Institute of Materials Science, University of Tsukuba, Tsukuba, Ibaraki 305-8573, Japan, and Department of Applied Biological Chemistry, Faculty of Agriculture, Osaka Prefecture University, 1-1 Gakuen-cho, Sakai, Osaka 599-8531 Japan

Received September 30, 2002; Revised Manuscript Received November 12, 2002

ABSTRACT: Photosynthetic water oxidation is performed via the light-driven S-state cycle in the water-oxidizing complex (WOC) of photosystem II (PS II). To understand its molecular mechanism, monitoring the reaction of substrate water in each S-state transition is essential. We have for the first time detected the reactions of water molecules in WOC throughout the S-state cycle by observing the OH vibrations of water using flash-induced Fourier transform infrared (FTIR) difference spectroscopy. Moderately hydrated (or deuterated) PS II core films from *Synechococcus elongatus* were used to obtain the FTIR difference spectra upon the first, second, third, and fourth flash illumination, representing the structural changes in the $S_1 \rightarrow S_2$, $S_2 \rightarrow S_3$, $S_3 \rightarrow S_0$, and $S_0 \rightarrow S_1$ transitions, respectively. In the weakly H-bonded OH region, bands appeared at 3617/3588 cm^{-1} as a differential signal in the first-flash spectrum and at 3634, 3621, and 3612 cm^{-1} with negative intensities in the second-, third-, and fourth-flash spectra, respectively. These bands shifted down by ∼940 cm^{-1} upon deuteration and by ∼10 cm^{-1} upon $H^{18}O$ substitution, indicating that they arise from the OH stretches of water including the substrate and its intermediates. Strongly D-bonded OD bands of water were also identified as broad features in the range of 2600−2200 cm^{-1} by taking the double difference between the spectra of $D_2{}^{16}O$- and $D_2{}^{18}O$-deuterated films. In addition, broad continuum features that probably arise from the large proton polarizability of H-bonds were observed around 3000, 2700, 2550, and 2600 cm^{-1} in the first-, second-, third-, and fourth-flash spectra, respectively, of the hydrated PS II film, revealing changes in the H-bond network of the protein. The negative OH intensities upon the second to fourth flashes might be related to proton release from substrate water. The results presented here showed that FTIR detection of water OH(D) bands can be a powerful method for investigating the mechanism of photosynthetic water oxidation.

Photosynthesis, which is performed by plants and certain types of bacteria, is a biological energy conversion process in which sugar and starch are synthesized from CO_2 using the energy of sunlight. As an ultimate source of electrons for reducing CO_2, plants and cyanobacteria utilize water, which is one of the most abundant resources on earth. Of additional significance in the water oxidation is that molecular oxygen is released as a byproduct. The oxygenic atmosphere of the earth relies on this photosynthetic oxygen evolution.

The reactions of water oxidation take place in the water-oxidizing complex (WOC),[1] which is located on the electron-donor side of photosystem II (PS II) (*1*−*3*). Although the catalytic core of WOC is known to consist of a tetranuclear Mn cluster, its structure still remains unclarified. A model of a dimer of di-μ-oxo dimers was proposed as one of the possible structures that explain the results of EXAFS studies (*3*, *4*), while detailed simulation of EPR signals by Peloquin et al. (*5*) preferred a trimer/monomer structure. The recent result of X-ray crystallography by Zouni et al. (*6*) was consistent with the trimer/monomer structure, although the resolution of 3.8 Å was not sufficient to draw an unequivocal conclusion. In WOC, two water molecules are oxidized to produce one O_2 molecule and four protons. Although this reaction is known to proceed through a flash-driven cycle of five intermediates, S_0−S_4, in which the S_1 state is dark stable and O_2 is released in the $S_4 \rightarrow S_0$ transition, its molecular mechanism largely remains a mystery.

To clarify the mechanism of water oxidation, spectroscopic methods for detecting the structures and reactions of substrate water are essential along with the effort to increase the resolution of the X-ray structure. In particular, because X-ray crystallography is weak in detecting hydrogen atoms, the reactions of water such as proton release and changes in H-bond interactions are hard to resolve with this method. To date, several methods have been applied to detect water or its reaction in WOC. The NMR relaxation rate of solvent protons was dependent on the S states, being attributed to the rapid equilibrium of the protons between bulk water and Mn-coordinated water (*7*). Mass spectrometric measurements

† This study was supported by Grant-in-Aid for Scientific Research 14540607 from the Ministry of Education, Culture, Sports, Science and Technology of Japan and by Special Research Project "Nano-Science" at the University of Tsukuba.

* To whom correspondence should be addressed. Phone: +81-298-53-5126. Fax: +81-298-55-7440. E-mail: tnoguchi@ims.tsukuba.ac.jp.

‡ University of Tsukuba.

§ Osaka Prefecture University.

[1] Abbreviations: FTIR, Fourier transform infrared; IR, infrared; Mes, 2-(*N*-morpholino)ethanesulfonic acid; PS II, photosystem II; WOC, water-oxidizing complex.

10.1021/bi020603i CCC: $22.00
Published on Web 12/07/2002

showed that the rate of ^{18}O incorporation has biphasic kinetics in all the S states, and thus, substrate water is bound at two different metal sites (*8*, *9*). CW EPR (*10*, *11*), ESEEM (*2*, *12*), and proton ENDOR (*13*, *14*) also provided evidence of the interaction of water with the Mn cluster. Resonance Raman spectra showed several low-frequency bands sensitive to D_2O-H_2O exchange in the S_1 state, which were temporally assigned to the $Mn-H_2O$ or $Mn-OH^-$ vibrations (*15*).

A more direct method of detecting water molecules will be infrared (IR) spectroscopy, because the OH stretching vibrations of water have strong IR absorption in the range of 3800−3000 cm^{-1}, in which the band frequencies reflect the structure and interaction of the water. IR studies of WOC started approximately 10 years ago, and light-induced Fourier transform infrared (FTIR) difference spectra of the $S_1 \rightarrow S_2$ transition were measured in the region of 1800−1000 cm^{-1}, in which the vibrations of amino acid side chains and protein backbones occur (*16*−*18*). The S_2/S_1 FTIR spectra have been used to study the structures of carboxylate (*16*−*22*) and histidine (*23*) ligands, and the interaction of a tyrosine residue with the Mn cluster (*24*). Chu et al. (*25*−*29*) further detected the S_2/S_1 spectra in the lower-frequency region of 1000−350 cm^{-1}, and assigned the 606/625 cm^{-1} signal to the Mn−O−Mn vibration by downshifts upon ^{18}O substitution (*27*). Recently, flash-induced FTIR difference spectra during the S-state cycle representing the changes in the $S_1 \rightarrow S_2$, $S_2 \rightarrow S_3$, $S_3 \rightarrow S_0$, and $S_0 \rightarrow S_1$ transitions were observed independently by Hillier and Babcock (*30*) and by us (*31*) using the PS II membranes of spinach and the core complexes of the cyanobacterium *Synochococcus elongatus*, respectively. It was shown that the structural changes in the carboxylate groups and protein backbones in the $S_1 \rightarrow S_2 \rightarrow S_3$ transitions were mostly reversed in the $S_3 \rightarrow S_0 \rightarrow S_1$ transitions (*31*).

FTIR bands of the OH stretching vibrations of water in WOC were first detected in the S_2/S_1 difference spectrum at 250 K (*32*). A differential signal was observed at 3618/3585 cm^{-1} in the weakly H-bonded OH region, and it exhibited downshifts upon D_2O and $H_2{}^{18}O$ substitution. From a decoupling experiment using an H_2O/D_2O (1:1) solution, it was proposed that this water molecule has an asymmetric structure in which one OH group is weakly H-bonded and the other strongly H-bonded, and that the asymmetry becomes larger upon formation of the S_2 state (*32*). In contrast to the weakly H-bonded OH bands, the strongly H-bonded OH region could not be detected due to the superimposition of the strong IR absorption of bulk water. In addition, attempts to detect the OH bands in other S-state transitions were not successful because the liquid PS II solution at 10 °C, the condition which was adopted to attain efficient S-state transitions in our previous study (*31*), exhibits water bands at higher frequencies than ice, which masked even the weakly H-bonded region (T. Noguchi and M. Sugiura, unpublished results).

We report here detection of the OH(D) stretching vibrations of water in WOC throughout the S-state cycle in both weakly and strongly H(D)-bonded OH(D) regions. To achieve this, we used moderately hydrated (or deuterated) PS II films in which the amount of water was significantly reduced so that IR absorption in the water OH region was not saturated (*33*). In such hydrated films, high efficiencies of the S-state transitions were retained (*33*). The observed signals reveal the reactions of water in WOC including substrate water, and hence provide direct information about the chemical mechanism of photosynthetic water oxidation.

MATERIALS AND METHODS

Oxygen-evolving PS II core complexes from *S. elongatus*, in which the carboxyl terminus of the CP43 subunit was genetically histidine-tagged, were purified using Ni^{2+} affinity column chromatography as described by Sugiura and Inoue (*34*). The PS II core complexes were suspended in 10 mM Mes-NaOH (pH 6.0) containing 5 mM NaCl, 5 mM $CaCl_2$, and 0.06% *n*-dodecyl β-D-maltoside and concentrated to ∼4.5 mg of Chl/mL using a Microcon-100 apparatus (Amicon). The sample solution was once dried under N_2 gas and resuspended in the same amount of $H_2{}^{16}O$ (natural abundance), $H_2{}^{18}O$ (Euriso-top, 95.44 at. % ^{18}O), $D_2{}^{16}O$ (CDN, 99.9 at. % D), and $D_2{}^{18}O$ (ICON, 99 at. % D, 85 at. % ^{18}O). This solvent exchange was repeated twice, and the sample was incubated overnight on ice for H_2O and at 6 °C for D_2O. For FTIR measurements, a water solution of 100 mM potassium ferricyanide (0.5 μL for the samples in H_2O and 1.0 μL for the samples in D_2O) was first dried on a CaF_2 window (25 mm × 3 mm), and then an aliquot of the core suspension (2 μL for H_2O and 4 μL for D_2O) was mixed with ferricyanide using a thin glass stick. Moderately hydrated (or deuterated) films of the PS II core complexes were prepared as reported previously (*33*) under the humidity control of the IR cell by enclosing 1 μL of a 40% (v/v) glycerol/water solution (note that the glycerol/water solution is placed in the IR cell so the solution does not touch the sample). At this time, glycerol/$H_2{}^{16}O$, glycerol/$H_2{}^{18}O$, glycerol$(OD)_3$ (CDN, 98.7 at. % D)/$D_2{}^{16}O$, and glycerol$(OD)_3$/$D_2{}^{18}O$ solutions were used for hydration (deuteration) with $H_2{}^{16}O$, $H_2{}^{18}O$, $D_2{}^{16}O$, and $D_2{}^{18}O$, respectively. Note that a smaller amount of sample was loaded for the hydrated films than the deuterated films for avoiding absorption saturation in the OH region. The average absorbances at major bands in the FTIR spectra of the samples were 0.70 at 3307 cm^{-1} (OH region) and 0.66 at 1657 cm^{-1} (amide I region) for the hydrated films, and 0.64 at 2500 cm^{-1} (OD region) and 0.88 at 1655 cm^{-1} (amide I′ region) for the deuterated films. The sample temperature was kept at 10 °C by circulating cold water in a copper holder.

Flash-induced FTIR difference spectra during the S-state cycle were recorded as reported previously (*33*) using a Bruker IFS-66/S spectrophotometer and a Q-switched Nd:YAG laser (Quanta-Ray GCR-130, 532 nm, ∼7 ns fwhm). Briefly, after two preflashes and subsequent dark adaptation for 1 h, the sample was subjected to four consecutive flashes with 10 s intervals. Single-beam spectra (10 s scan) were recorded before and after each flash. The sample was then dark-adapted for 1 h, and this cycle was repeated up to 16 times for one sample. Difference spectra (after minus before the flash) were calculated for each flash, and the spectra recorded with several samples were averaged. All spectra were recorded with a resolution of 4 cm^{-1}.

RESULTS

Figure 1 (red lines) shows flash-induced FTIR difference spectra in the 1800−1200 cm^{-1} region of a moderately hydrated PS II core film of *S. elongatus* measured at 10 °C.

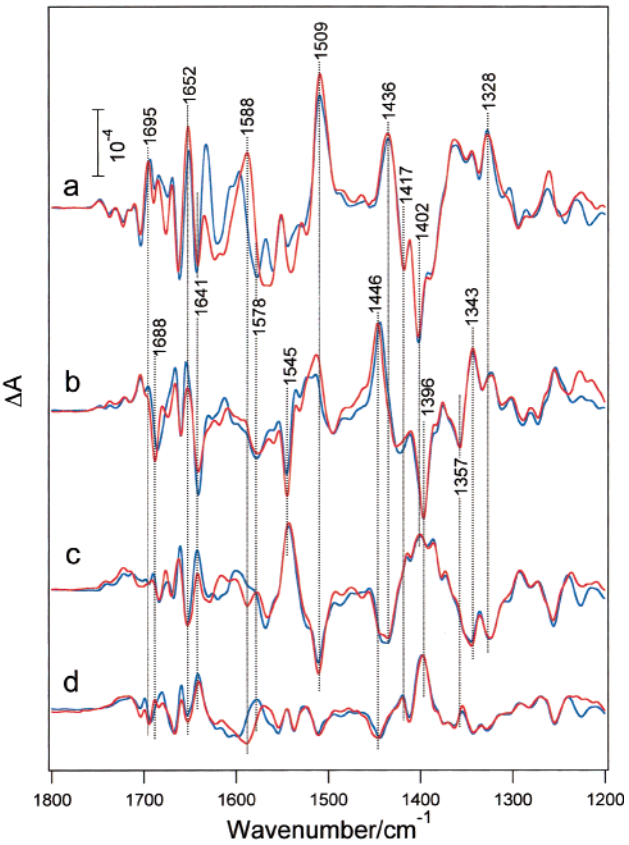

FIGURE 1: Flash-induced FTIR difference spectra (1800−1200 cm^{-1}) of WOC upon (a) first-, (b) second-, (c) third-, and (d) fourth-flash illumination on the PS II core films moderately hydrated with H_2O (red lines) and deuterated with D_2O (blue lines). The PS II samples include ferricyanide as an electron acceptor, and the sample temperature was 10 °C. The Δ*A* intensity expressed in the figure represents that of the spectra of the hydrated film. The spectra of the deuterated film were scaled to adjust the intensities to those of the hydrated film. The data of the hydrated and deuterated films were the average of 72 spectra (1440 interferograms) and 120 spectra (2400 interferograms), respectively.

Bands in this region mostly arise from the vibrations of protein backbones and side chains. The spectra were basically identical to those we previously reported, and the first-, second-, third-, and fourth-flash spectra virtually represent the structural changes that occur with the $S_1 \rightarrow S_2$, $S_2 \rightarrow S_3$, $S_3 \rightarrow S_0$, and $S_0 \rightarrow S_1$ transitions, respectively (*33*). Prominent features are the bands in the symmetric and asymmetric stretching regions of caroboxylate groups in the 1450−1300 and 1600−1500 cm^{-1} regions, respectively, and the amide I bands in the 1700−1600 cm^{-1} region and the amide II bands around 1550 cm^{-1}. Major bands in the first- and second-flash spectra have corresponding counter bands at the same positions but with opposite signs in the third- and fourth-flash spectra (Figure 1), suggesting that the protein movements in the $S_1 \rightarrow S_2 \rightarrow S_3$ transitions are reversed in the $S_3 \rightarrow S_0 \rightarrow S_1$ transitions in the catalytic cycle (*31*). Flash-induced spectra of the deuterated PS II film are also shown in Figure 1 (blue lines). An upshifted band in the asymmetric COO^- stretching region in the first-flash spectrum, a typical effect of deuteration on the S_2/S_1 spectrum reported previously (*18*), was clearly seen at 1578 cm^{-1}, and its counter band was found at the same position in the fourth-flash spectrum (Figure 1). Some other bands were also sensitive to H−D exchange. A detailed analysis of the isotope effects in this region will be discussed elsewhere.

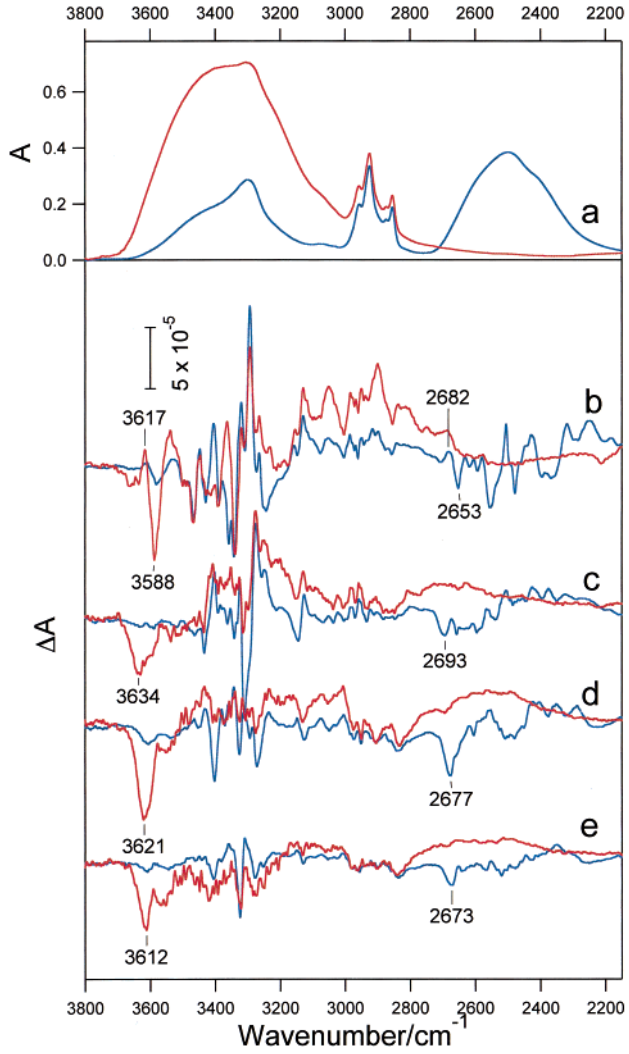

FIGURE 2: High-frequency region (3800−2150 cm^{-1}) of the FTIR absorption spectra (a) and the flash-induced difference spectra of WOC upon (b) first-, (c) second-, (d) third-, and (e) fourth-flash illumination of the moderately hydrated (red lines) and deuterated (blue lines) PS II core films. The absorbance and Δ*A* intensity expressed in the figure represent those of the spectra of the hydrated film, and the spectra of the deuterated film were scaled with the same factors as for the 1800−1200 cm^{-1} region in Figure 1.

In Figure 2 is shown the higher-frequency region (3800−2150 cm^{-1}) of the flash-induced difference spectra of the hydrated (red lines) and deuterated (blue lines) PS II films (b and c) together with their absorption spectra (a). The spectra of the deuterated film were scaled so that the intensities of the difference spectra in the 1800−1200 cm^{-1} region were adjusted to those of the hydrated film (Figure 1). In the absorption spectrum of the hydrated film (Figure 2a, red line), the OH stretching bands of H_2O appeared around 3400 cm^{-1}, superimposed on the bands of the OH and NH stretches of the protein backbones and side chains around 3300 cm^{-1}. The sharp bands at 3000−2800 cm^{-1} are due to the CH stretches of the CH_2 and CH_3 groups. In the deuterated PS II film (Figure 2a, blue line), the OD stretches of D_2O showed a band around 2500 cm^{-1}. Note that the lower intensity of this OD band compared with that of the OH band around 3400 cm^{-1} is attributed to the extinction coefficient of the OD stretch being originally smaller than that of the OH stretch (*35*). The band around

2500 cm^{-1} also includes the OD and ND stretches of the exchangeable OH and NH groups of the protein. Bands of nonexchangeable OH and NH groups in hydrophobic domains of the protein remained around 3300 cm^{-1} in the spectrum of the deuterated film (Figure 2a, blue line).

Flash-induced spectra of the hydrated film (Figure 2b−e, red lines) showed clear peaks in the weakly H-bonded OH region around 3600 cm^{-1}, which is present under the high-frequency edge of the OH band of the absorption spectrum (Figure 2a). The differential signal at 3617/3588 cm^{-1} in the first-flash spectrum (Figure 2b, red line) corresponds to the 3618/3585 cm^{-1} signal previously reported for the PS II core solution at 250 K (*32*). The second-, third-, and fourth-flash spectra in this region showed negative features with different peak positions depending on the flash number: 3634, 3621, and 3612 cm^{-1} for the second, third, and fourth flash, respectively. All of these bands disappeared or were significantly reduced in intensity upon deuteration (Figure 2b,c, blue lines). Instead, bands with similar shapes appeared in the weakly D-bonded OD region at 2682/2653, 2693, 2677, and 2673 cm^{-1} in the first-, second-, third-, and fourth-flash spectra, respectively. The lower intensities of these OD bands compared with the intensities of the corresponding OH bands are again consistent with the extinction coefficient of OD being smaller than that of the OH stretch.

Some sharp bands were observed in 3500−3000 cm^{-1} region in all the flash-induced spectra of the hydrated film (Figure 2b−e, red lines). However, these bands mostly remained even after deuteration (Figure 2b−e, blue lines), indicating that these originate from nonexchangeable OH or NH groups of the protein in a hydrophobic environment. This observation suggests that a large fraction of the groups at the active site of WOC is present in hydrophobic protein moieties. Broad positive features were observed around 3000, 2700, 2550, and 2600 cm^{-1} in the first-, second-, third-, and fourth-flash spectra, respectively, of the hydrated PS II film (Figure 2b−e, red lines). These features diminished in intensity upon deuteration (Figure 2b−e, blue lines), indicating a relationship with exchangeable protons. Also, the frequencies of these features, especially of the latter three, were much lower than those of usual H-bonded OH and NH bands [>3000 cm^{-1} (*36*)]. Hence, these broad features most probably arise from IR absorption by the large proton polarizability of strong H-bonds, which is known as Zundel polarizability (*37*). Similar continuum bands due to highly polarizable H-bonds have been observed in the Q_A^-/Q_A and Q_B^-/Q_B difference spectra of bacterial reaction centers (*38*). The appearance of these broad bands in the flash-induced spectra with different positions depending on the flash number indicates that the proton polarizability in the H-bond network around the Mn cluster changes during the S-state cycle. Sharp peaks with medium or weak intensities observed in the 3000−2800 cm^{-1} region in both the hydrated and deuterated films may arise from the CH stretches of the protein.

Expanded spectra in the weakly H-bonded OH region (3700−3500 cm^{-1}) of the hydrated films and in the whole OD region (2800−2150 cm^{-1}) of the deuterated films are presented in Figures 3 and 4, respectively. Note that the signal-to-noise ratio in the entire OD region was much better than in the OH region (compare the blue lines in the 2800−2150 cm^{-1} region with the red lines in the 3800−3000 cm^{-1} region in Figure 2b−e) because of the higher sensitivity of the MCT detector in the OD region and less superimposition of the protein bands. In the weakly D-bonded region (2800−2600 cm^{-1}), minor structures were clearly observed along with the major peaks mentioned above, for example, a negative peak at 2707 cm^{-1} at the first flash, a differential signal at 2673/2657 cm^{-1} at the second flash, and a positive peak at 2652 cm^{-1} at the fourth flash (Figure 4). These minor OD peaks probably correspond, in the hydrated film, to a negative feature at 3664 cm^{-1} at the first flash, a broad negative feature at ∼3600 cm^{-1} at the second flash, and a positive shoulder at 3591 cm^{-1} at the fourth flash, respectively (Figure 3). The major peaks in the weakly H-bonded OH region of 3700−3500 cm^{-1} together with minor features all shifted down by ∼10 cm^{-1} upon hydration with $H_2{}^{18}O$ (Figure 3). Similarly, both the major and minor peaks in the weakly D-bonded OD region of 2800−2600 cm^{-1} downshifted upon deuteration with $D_2{}^{18}O$ (Figure 4). These results indicate that the bands observed in the weakly H(D)-bonded OH(D) region originate from OH(D) vibrations of water or its intermediates. Although in the lower-frequency OD region (2600−2200 cm^{-1}) some moderately sharp structures were observed (Figure 4, thick lines), they were not sensitive to $D_2{}^{18}O$ substitution (Figure 4, thin lines) except for the peaks at 2555 cm^{-1} at the first flash and at 2557 cm^{-1} at the third flash. Thus, they are mostly due to the OD and/or ND groups of the protein in a hydrophilic environment.

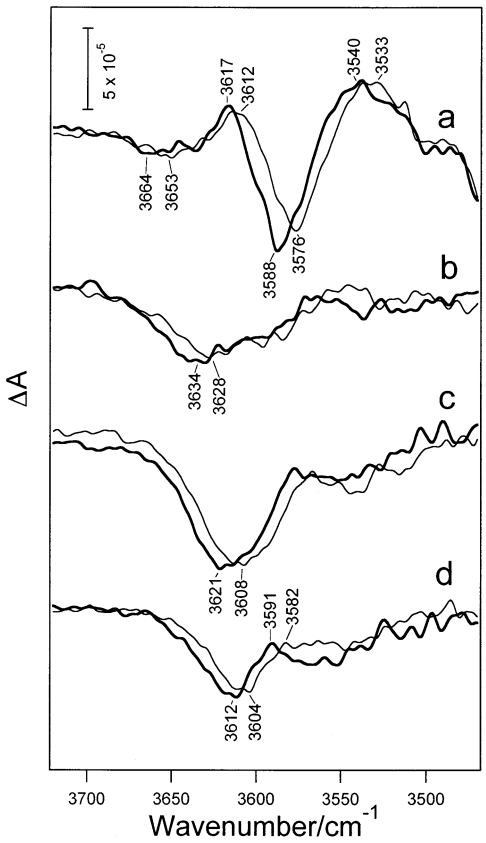

FIGURE 3: Expanded view of the weakly H-bonded OH stretching region (3700−3500 cm^{-1}) of the FTIR difference spectra of WOC upon (a) first-, (b) second-, (c) third-, and (d) fourth-flash illumination on the PS II core films hydrated with $H_2{}^{16}O$ (thick lines) and $H_2{}^{18}O$ (thin lines).

It is known that as an OH(D) group of water is more strongly H(D)-bonded, the OH(D) stretching band appears

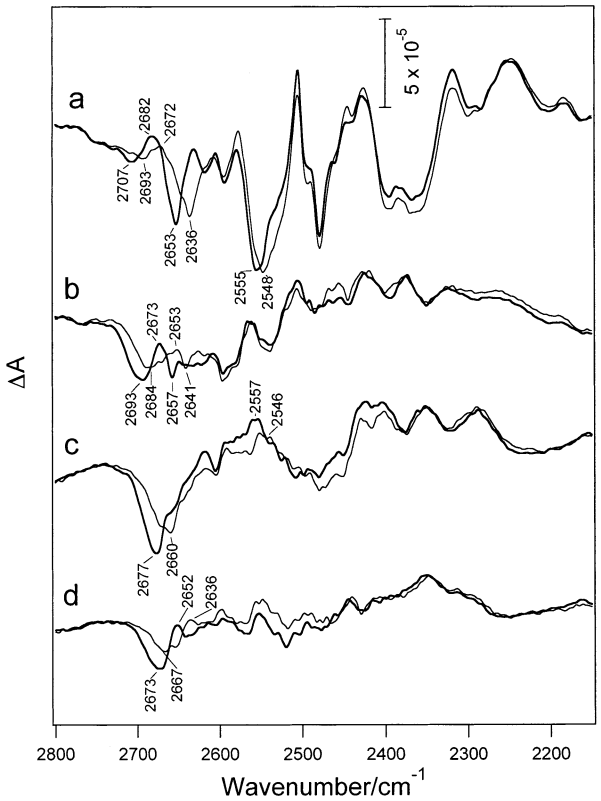

FIGURE 4: FTIR difference spectra of WOC in the OD stretching region (2800−2150 cm^{-1}) upon (a) first-, (b) second-, (c) third-, and (d) fourth-flash illumination on the PS II films deuterated with $D_2{}^{16}O$ (thick lines) and $D_2{}^{18}O$ (thin lines).

at a lower frequency with a broader bandwidth (*39*). In the flash-induced spectra of the PS II films, broad OH(D) bands due to strong H(D) bonding should be present in the lower-frequency region of <3500 cm^{-1} (<2600 cm^{-1}). However, these broad features are difficult to recognize in the presence of other OH(D) and NH(D) bands of the protein. To abstract only water bands from the flash-induced spectra, double-difference spectra at each flash (Figure 5) were calculated between the spectra of the PS II films deuterated with $D_2{}^{16}O$ (Figure 4, thick lines) and with $D_2{}^{18}O$ (Figure 4, thin lines). The spectra of the deuterated films were used for calculation because of a higher signal-to-noise ratio in the OD region than in the OH region (see above) that gives a more reliability of the data. The resultant spectra in Figure 5 provide only the signals of water and/or its intermediates that change upon each S-state transition. The sharp structures in the 2750−2600 cm^{-1} region are due to the weakly D-bonded OD stretches already mentioned. In the 2600−2200 cm^{-1} region, medium or broad features were observed at every flash, and these arise from the strongly D-bonded OD stretches of water. The lower-frequency features are thought to be due to stronger D-bonded OD groups. This view is supported by the observation that the bands were broader at the lower frequencies (Figure 5) as expected from the general correlation between the frequency and the bandwidth of an OH(D) stretch (*39*).

DISCUSSION

In this study, we have identified IR absorption bands of water in the flash-induced FTIR difference spectra of WOC during the S-state cycle. The bands in the weakly H-bonded

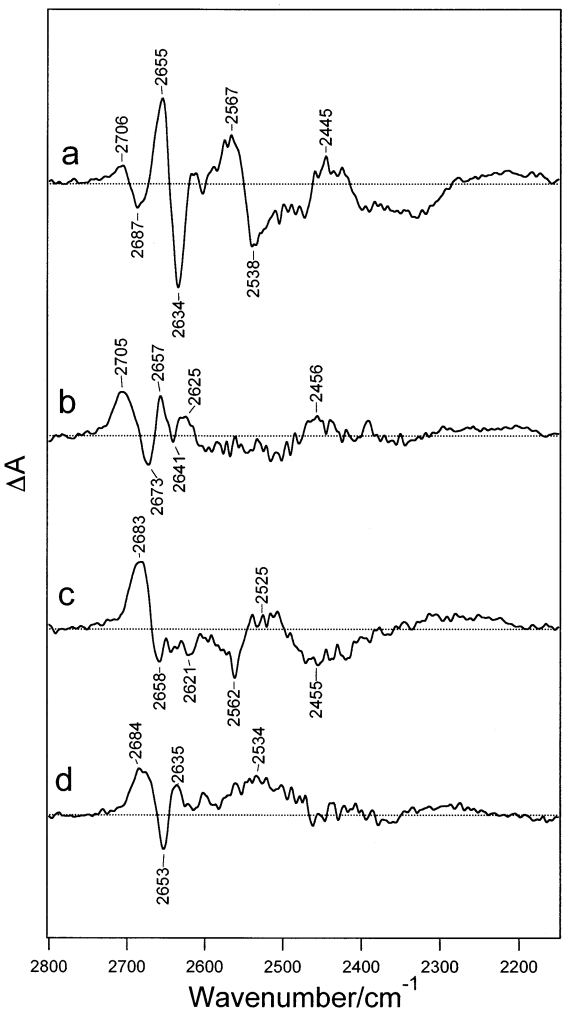

FIGURE 5: Double-difference spectra ($D_2{}^{18}O - D_2{}^{16}O$) in the OD stretching region (2800−2150 cm^{-1}) upon (a) first-, (b) second-, (c) third-, and (d) fourth-flash illumination. The difference spectrum of the $D_2{}^{16}O$-deuterated film at each flash (Figure 4, thick lines) was subtracted from that of the $D_2{}^{18}O$-deuterated film (Figure 4, thin lines) to cancel the bands in the 1800−1200 cm^{-1} region as much as possible.

OH stretching region of 3800−3500 cm^{-1} were definitely assigned to the OH vibrations of water and/or its intermediates by downshifts by ∼940 cm^{-1} upon deuteration and by ∼10 cm^{-1} upon $H^{18}O$ substitution (Figures 2 and 3). Despite the fact that the main feature in the first-flash spectrum (i.e., S_2/S_1) was a differential signal at 3617/3588 cm^{-1}, the second-, third-, and fourth-flash spectra (i.e., S_3/S_2, S_0/S_3, and S_1/S_0, respectively) exhibited negative features at frequencies specific to individual S-state transitions (Figure 3). The peak frequencies were in the order of the second (3634 cm^{-1}), third (3621 cm^{-1}), and fourth (3612 cm^{-1}) flash, and the negative peak at the first flash exhibited the lowest frequency (3588 cm^{-1}). The characteristics of these band shapes and the frequency order were reproduced in the weakly D-bonded OD bands of the deuterated PS II film (Figure 4). A differential signal was observed at 2682/2653 cm^{-1} at the first flash, and negative bands appeared in the frequency order of the second (2693 cm^{-1}), third (2677 cm^{-1}), and fourth (2673 cm^{-1}) flashes.

In the 1800−1200 cm^{-1} region of protein vibrations, a band observed at a certain flash has a counter band at the same frequency but with the opposite sign at another flash

(Figure 1) (*31*), reflecting the catalytic role of the protein in WOC. However, such band correspondence was not explicitly seen in the water OH(D) bands, although the negative band at 3621(2677) cm^{-1} at the third flash could include a contribution of the counter band of the positive peak at 3617(2682) cm^{-1} at the first flash and the positive shoulder at 3591(2652) cm^{-1} at the fourth flash might correspond to the negative peak at 3588(2653) cm^{-1} at the first flash. If the observed OH(D) bands arise from the water molecules that are not substrates but simply structural constituents of WOC, the counter bands should be found at another transition like the protein bands. Thus, this observation and the predominance of the negative intensities are consistent with the idea that the identified water bands include those of substrate water of WOC, which should be consumed during the S-state cycle.

Among the negative features of the weakly H(D)-bonded OH(D) bands at the second, third, and fourth flashes, the intensity at the third flash is larger than that at the other flashes by a factor of ~2 (Figures 3 and 4). Hence, the intensity ratio of the OH(D) signal is roughly deduced as 0 (differential signal), 1, 2, and l at the first, second, third, and fourth flashes, respectively. This intensity relationship seems to be correlated with the reported proton release pattern, 0.2:1.0:1.8:1.0 for the $S_1 \rightarrow S_2 \rightarrow S_3 \rightarrow S_0 \rightarrow S_1$ transitions, of the PS II core complexes of *S. elongatus* at pH 6.0 (*40*), although more quantitative analysis will require accurate correction of the spectra using miss factors. Thus, it might be possible that the observed bleaching of the water OH(D) bands could be directly related to the proton release reactions. In this case, protons do not need to be released directly from the weakly H-bonded OH groups. Strongly H-bonded OH groups may actually undergo proton release, and then the weakly H-bonded OH groups are newly engaged in strong H-bonding.

We previously suggested that the water molecule in which one OH group is weakly H-bonded showing the 3618/3585 cm^{-1} feature in the S_2/S_1 spectrum has a highly asymmetric structure and the other OH group of this water is strongly H-bonded (*32*). This idea was recently verified by Fischer and Wydrzynski (*41*) in their theoretical calculations considering the coupling between the two OH stretching modes of the water. They predicted that the frequency of the counter OH band coupled to the observed OH at 3585 cm^{-1} is 3366 cm^{-1} [by the density functional theory (DFT) method] or 3392 cm^{-1} [by the Hartree−Fock (HF) method] and that the OD frequency coupled to the observed OD band at 2652 cm^{-1} is 2370 cm^{-1} (DFT) or 2432 cm^{-1} (HF) (*41*). In this study, strongly D-bonded OD bands of water were detected in the 2600−2200 cm^{-1} region as broad features by calculating double-difference spectra between the $D_2{}^{16}O$- and $D_2{}^{18}O$-deuterated films (Figure 5). The possible candidate for the strongly D-bonded OD band coupled to the 2652 cm^{-1} band (2653 cm^{-1} in this study) in the S_1 state is a positive feature at 2445 cm^{-1} observed in the double-difference spectrum at the first flash (Figure 5a).

Changes in the H-bond network during the S-state cycle were expressed in the appearance of the broad features in the 3000−2200 cm^{-1} region in the flash-induced spectra of the hydrated film (Figure 2, red lines). These features were attributed to the high proton polarizability in the H-bond network, which generally plays a crucial role in proton transfer reactions in proteins (*37*). Thus, the appearance of the bands in the difference spectra can be caused by the proton release reactions in WOC. Proton polarizability is also affected by local electrical fields (*37*), and hence, this IR absorption might be coupled to the redox changes of the Mn cluster. The central frequencies of the broad positive features were dependent on the flash number, i.e., 3000, 2700, 2550, and 2600 cm^{-1} at the first, second, third, and fourth flashes, respectively (Figure 2, red lines). The observation that the second, third, and fourth flashes exhibited much lower frequencies than the first flash and the frequency at the third flash is the lowest among them could be again related to the proton release pattern for individual S-state transitions (*40*), because more protons in the system would make stronger H-bond networks, providing lower-frequency continuum bands. The relatively large positive feature at the first flash might be caused by putative oxidation of the Mn cluster in the $S_1 \rightarrow S_2$ transition (*1*).

In conclusion, the reactions of water during the flash-induced S-state cycle of WOC were for the first time monitored by detecting the OH(D) stretching vibrations by means of FTIR spectroscopy using moderately hydrated (deuterated) PS II core films. The observed signals should reflect basically all the reactions of substrate water, including proton release, changes in H-bond interactions, and binding to the Mn ion. A detailed analysis of these signals in combination with site-directed mutagenesis and various perturbations to the WOC will provide important information for understanding the molecular mechanism of photosynthetic water oxidation.

REFERENCES

1. Debus, R. J. (1992) *Biochim. Biophys. Acta 1102*, 269−352.
2. Britt, R. D. (1996) in *Oxygenic Photosynthesis*: *The Light Reactions* (Ort, D. R., and Yocum, C. F., Eds.) pp 137−164, Kluwer, Dordrecht, The Netherlands.
3. Yachandra, V. K., Sauer, K., and Klein, M. P. (1996) *Chem. Rev. 96*, 2927−2950.
4. Yachandra, V. K., DeRose, V. J., Latimer, M. J., Mukerji, I., Sauer, K., and Klein, M. P. (1993) *Science 260*, 675−679.
5. Peloquin, J. M., Campbell, K. A., Randall, D. W., Evanchik, M. A., Pecoraro, V. L., Armstrong, W. H., and Britt, R. D. (2000) *J. Am. Chem. Soc. 122*, 10926−10942.
6. Zouni, A., Witt, H. T., Kern, J., Fromme, P., Krauss, N., Saenger, W., and Orth, P. (2001) *Nature 409*, 739−743.
7. Sharp, R. R. (1992) in *Manganese Redox Enzymes* (Pecoraro, V. L., Ed.) pp 177−196, VCH Publishers, New York.
8. Hillier, W., Messinger, J., and Wydrzynski, T. (1998) *Biochemistry 37*, 16908−16914.
9. Hillier, W., and Wydrzynski, T. (2000) *Biochemistry 39*, 4399−4405.
10. Hansson, Ö., Andréasson, L.-E., and Vänngard, T. (1986) *FEBS Lett. 195*, 151−154.
11. Nugent, J. H. A. (1987) *Biochim. Biophys. Acta 893*, 184−189.
12. Evans, M. C. W., Rich, A. M., and Nugent, J. H. A. (2000) *FEBS Lett. 477*, 113−117.
13. Kawamori, A., Inui, T., Ono, T., and Inoue, Y. (1989) *FEBS Lett. 254*, 219−224.
14. Fiege, R., Zweygart, W., Bittl, R., Adir, N., Renger, G., and Lubitz, W. (1996) *Photosynth. Res. 48*, 227−237.
15. Cua, A., Stewart, D. H., Reifler, M. J., Brudvig, G. W., and Bocian, D. F. (2000) *J. Am. Chem. Soc. 122*, 2069−2077.
16. Noguchi, T., Ono, T., and Inoue, Y. (1992) *Biochemistry 31*, 5953−5956.
17. Noguchi, T., Ono, T., and Inoue, Y. (1995) *Biochim. Biophys. Acta 1228*, 189−200.
18. Noguchi, T., Ono, T., and Inoue, Y. (1995) *Biochim. Biophys. Acta 1232*, 59−66.

19. Noguchi, T., Sugiura, M., and Inoue, Y. (1999) in *Fourier Transform Spectroscopy* (Itoh, K., and Tasumi, M., Eds.) pp 459−460, Waseda University Press, Tokyo, Japan.
20. Kimura, Y., and Ono, T. (2001) *Biochemistry 40*, 14061−14068.
21. Kimura, Y., Hasegawa, K., and Ono, T. (2002) *Biochemistry 41*, 5844−5853.
22. Chu, H.-A., Babcock, G. T., and Debus, R. J. (2001) in *Proceedings of the 12th International Congress on Photosynthesis*, S13-026, CSIRO Publishing, Collingwood, Australia.
23. Noguchi, T., Inoue, Y., and Tang, X.-S. (1999) *Biochemistry 38*, 10187−10195.
24. Noguchi, T., Inoue, Y., and Tang, X.-S. (1997) *Biochemistry 36*, 14705−14711.
25. Chu, H.-A., Gardner, M. T., O'Brien, J. P., and Babcock, G. T. (1999) *Biochemistry 38*, 4533−4541.
26. Chu, H.-A., Hillier, W., Law, N. A., and Babcock, G. T. (2000) *Biochim. Biophys. Acta 1503*, 69−82.
27. Chu, H.-A., Sackett, H., and Babcock, G. T. (2000) *Biochemistry 39*, 14371−14376.
28. Chu, H.-A., Gardner, M. T., Hillier, W., and Babcock, G. T. (2001) *Photosynth. Res. 66*, 57−63.
29. Chu, H.-A., Debus, R. J., and Babcock, G. T. (2001) *Biochemistry 40*, 2312−2316.
30. Hillier, W., and Babcock, G. T. (2001) *Biochemistry 40*, 1503−1509.
31. Noguchi, T., and Sugiura, M. (2001) *Biochemistry 40*, 1497−1502.
32. Noguchi, T., and Sugiura, M. (2000) *Biochemistry 39*, 10943−10949.
33. Noguchi, T., and Sugiura, M. (2002) *Biochemistry 41*, 2322−2330.
34. Sugiura, M., and Inoue, Y. (1999) *Plant Cell Physiol. 40*, 1219−1231.
35. Venyaminov, S. Y., and Prendergast, F. G. (1997) *Anal. Biochem. 248*, 234−245.
36. Socrates, G. (1994) in *Infrared Characteristic Group Frequencies*, 2nd ed., John Wiley & Sons, Chichester, U.K.
37. Zundel, G. (1988) *J. Mol. Struct. 177*, 43−68.
38. Breton, J., and Nabedryk, E. (1998) *Photosynth. Res. 55*, 301−307.
39. Luck, W. A. P., Klein, D., and Rangsriwatananon, K. (1997) *J. Mol. Struct. 416*, 287−296.
40. Schlodder, E., and Witt, H. T. (1999) *J. Biol. Chem. 274*, 30387−30392.
41. Fischer, G., and Wydrzynski, T. (2001) *J. Phys. Chem. B 105*, 12894−12901.

BI020603I